Sub-hourly Error Analysis of Decomposition-Transposition Model Pairs for Temperate Climates

Yazan J.K. Musleh [1], Willow Herring [1], Carlos D. Rodríguez-Gallegos [2], Stuart A.Boden [1] and Tasmiat Rahman [1]
[1] University of Southampton, University Road, Southampton, SO17 1BJ, Hampshire, United Kingdom
[2] RINA Tech Renewables Australia, RINA Consulting, Melbourne VIC 3000, Australia

Abstract — Feasibility software for photovoltaic (PV) systems leverage decomposition-transposition model pairs to approximate Plane-of-Array (POA) irradiance. This study analyses the accuracy of 15 optical model pairs, using minute input irradiance, to assess POA predictions in a temperate setting by comparing to measured POA for both an actuator-based tracker and a 55° south-facing tilted system. Using the Mean Absolute error (MAE) of ≤5% as the benchmark, significant variations were revealed across diverse sky conditions. Model estimates showcased a broad range of errors from the measured data, from 2.67% to 51.07%, influenced by variables such as K_t and system type. For the tracking system, the evaluation showed that in clear conditions, ten model pairs maintained errors within the range. However, this success diminished under intermediate skies, with only five models remaining within range, and further reduced to two models in overcast conditions. The fixed tilt system demonstrated similar trends but with fewer models meeting the required thresholds; four models in clear conditions, and only two in intermediate conditions. Remarkably, only the DISC-SO model pair met the threshold in overcast conditions, exhibiting an MAE of 2.67%. Thus, the DISC-SO model pair consistently met the threshold for both systems under all conditions, making it a preferred choice for transposing horizontal irradiance. However, R^2 values (0.5034, 0.5379, 0.5083 for clear, intermediate, and overcast conditions, respectively) highlighted challenges due to the high temporal resolution of input data and the hourly data-based SO transposition model. Moreover, the study also examined the impact of decomposition and transposition models on percentage errors. Decomposition changes caused discrepancies of up to 2.43% for tracking systems and 5.34% for fixed-tilt systems. In contrast, transposition model changes resulted in errors of 8.53% and 11.51%, respectively. Additionally, using hourly solar irradiance data yielded lower errors compared to minute data, with 1.44% in intermediate conditions, -2.15%, and 2.35% in overcast and clear conditions, likely due to the models being developed empirically with hourly data.

***Index Terms*— Solar irradiance, Temperate Climates, Sky Clearness Index, Decomposition Models, Transposition Models.**

I. INTRODUCTION

According to the 2022 IPCC report, the goal of maintaining global warming below 1.5 °C is contingent on two factors: a 45% reduction in carbon emissions before 2030, and renewable energy sources supplying between 70% and 85% of power by 2050 [1][2]. Consequently, the British energy security policy commits to increasing solar energy deployment by fivefold to 70 GW by 2035 [3]. For enhancing the deployment of photovoltaic (PV) systems, it is critical to minimize the error in PV simulation software (herein after named feasibility software). Primarily, this involves the task of validating the mathematical models embedded within these software solutions, particularly in temperate climate zones where the empirical nature of such models becomes paramount. These mathematical constructs serve a pivotal role in estimating the Plane-of-Array (POA) irradiance; the amount of sunlight available for collection at a particular panel orientation.

Thus, an accurate appraisal of PV performance is central to the economic viability of systems [6]. The large variety of model pairs available can introduce error and therefore increase risk in the PV deployment process. Feasibility software offers a multitude of model combinations, but there is no established standard for their use [22]. Previous research indicate that applying the same meteorological information and system definitions can lead to differing POA irradiance predictions [49]. POA is crucial for making knowledgeable choices, spanning various domains from analyzing shade effects to assessing economic feasibility.

The International Technology Roadmap for Photovoltaic (ITRPV) estimates that by 2030, 40% of photovoltaic (PV) systems will incorporate tracking technologies [4]. Reinforcing this, the International Energy Agency (IEA) highlights the growing use of single-axis trackers in the USA, surpassing Fixed-Tilt (FT) systems within PV farms. Moreover, it demonstrates the growing global market for PV trackers. The pursuit of tracking technologies in the PV landscape holds the potential for enhanced energy output and therefore reduction in the number of modules required per kWh [5][43]. However, tracking solutions in PV systems often necessitate increased physical space, which could be a hurdle in space-limited areas [54]. Therefore, precise modelling is essential to ensure that the benefits provided by these solutions surpass their spatial needs. Furthermore, the use of trackers introduces concerns about return on investment [6].

The economic viability of PV systems, be they categorized as FT or tracking, largely relies on accurate POA estimations. This evaluation is typically executed using a view-factor method [6], implemented through feasibility software. At present, satellite imagery is employed to collect Global Horizontal Irradiance (GHI) [47], which is then separated into its direct and diffuse components (Direct Normal Irradiance (DNI) and Diffuse Horizontal Irradiance (DHI)) through decomposition models. These models, through mathematical regression, use empirical constants and differing parameters [7]. Transposition models, which draw on empirical data at different tilts (β) and system azimuth (ψ_{system}) from diverse latitudes (φ) and periods, further this process by predicting POA [8][48]. Different software utilise combinations of these models – a list of commonly used model pairs is given in Table 1.

Transposition models can be divided into two categories: isotropic and anisotropic. Isotropic models depict Diffuse Horizontal Irradiance (DHI) as a consistent distribution of rays across the entire sky dome, signifying equal irradiance in every direction. On the other hand, anisotropic models (e.g. Perez [14]), are considerably more intricate as they break away from the restrictive assumption of complete isotropy. They divide solar irradiance into distinct elements: circumsolar (rays within a spherical cone

with a 25° half angle), and horizon brightening (rays emanating from a planar beam) built on top of an isotropic foundation. Therefore, during the incorporation of both decomposition and transposition models, as carried out in feasibility software, errors tends to escalate. This is attributable to a cascading effect where an underestimated DHI stemming from decomposition models, could result in an overestimated DNI, and subsequently, POA when these irradiance components are transposed. Conversely, an overestimated DHI would yield the opposite behaviour.

II. Literature Review

There are numerous studies evaluating decomposition-transposition model pairs. For example, Lave et al. examined two model pairs across 9 locations in the US for FT systems (predominantly with a south-facing β = 25°), concluding that regardless of the decomposition model used, the choice of transposition model resulted in differing outcomes; the Hay model showed less error compared to its Perez counterpart [23]. In their research, Sun et al. implemented the Orgill and Hollands decomposition model [50], coupled with the Perez transposition model. Their validation exercises focused solely on FT systems set at β = 15° and 30° at φ = 35°, revealing a variation in modelled irradiance Bifacial Gain (BG) of 6.40% compared to measurements [24]. Furthermore, the DIRINT-Perez model pairing was leveraged in an additional investigation [6], wherein Levelised Cost of Electricity calculations served as a validation criterion. An identical model pairing was used across six locations for an irradiance BG study [25].

The collection of 6 sites involved a Single Axis Tracker (SAT) and south-facing FT at φ = 35°, resulting in a 6% error from modelled BG. The setup at location 2 compromised an FT system of β = 34°, supplemented by two SATS at φ = 37.5°, resulting in a 5% error from the model. Location 3 was near the equator and featured a 10° β. Location 4 maintained β=24°, identical to its φ, whereas location 5 (φ = 51°) featured an FT setup with β = 35°. The BG from locations 3, 4, and 5 showed considerable consistency with the model, displaying errors of only 1%, 3.16%, and 1.65% respectively.

Yang et al. assessed ten transposition and five decomposition models under tropical conditions at φ = 1.3°. It was discovered that combining both types of models leads to increased prediction errors when converting irradiance from horizontal to tilted surfaces, with the error magnifying as β increases. This highlights the need to explore the percentage error in the modelling results at higher tilts, which is important for bifacial systems or monofacial systems requiring greater β for optimal incident angle [52]. Maani et al. noted that limiting studies to a single model combination might result in less accurate model chain indicators [55]. Roberts et al conducted a year-long study at φ = 52.7°, analyzing 16 pairs of optical models using hourly data. Their research highlighted that the DISC decomposition model paired with the Liu-Jordan isotropic model delivered superior accuracy compared to other combinations; validated on a FT system (β = 45° with ψ_{system} of 12° relative to the South). It was recommended that future research delve into the empirical derating factors employed in PV modeling today, considering diverse system configurations with various β -ψ_{system} combinations [56].

Despite these findings, it is notable that the majority of the optical model pair validation studies use hourly data and FT systems. This leaves a knowledge gap concerning their utility for a range of angles, a prerequisite for tracking systems, along with a higher temporal resolution and under temperate climates. Additionally, Gueymard showed that most of the error in predicting POA irradiance at a sunny location stems from the empirical separation of direct and diffuse components when these are not measured locally [51]. Hofmann et al. noted that decomposition models tend to produce a broader range of outcomes, whereas transposition models significantly influence these results. Nevertheless, additional validation is necessary for areas with diffuse climates, and a range of β needs to be considered [53]. These findings raise a critical question about whether similar conclusions can be drawn for locations with high levels of diffuse light, and which has a greater impact on POA irradiance: the decomposition or the transposition aspect.

Table 1: Various model pairs deployed in different feasibility software [44][45].

Decomposition Model	Transposition Model	Abbreviation	Software
Erbs [9]	Perez [14]	Erbs-Perez	INSEL [34] PVSYST [33]
	Liu-Jordan [15]	Erbs-LJ	PVToolbox [36] INSEL [34] RETScreen [35]
	Skartveit-Olseth [16] Temps-Coulson [17] Willmot [18] Bugler [19]	Erbs-SO Erbs-TC Erbs-Willmot Erbs-Bugler	INSEL [34]
	Hay [20]	Erbs-Hay	PVSYST [33] INSEL [34]
Reindl [10]	Perez [14]	Reindl-Perez	PVSOL [42] TRNSYS [37]
	Skartveit-Olseth [16] Hay [21]	Reindl-SO Reindl-Hay	PVSOL [42] TRNSYS [37]
DIRINT [11]	Perez [14]	DIRINT-Perez	SolarAnyWhere [38] SolarGIS [39]
DISC [12]	Hay [21] Perez [14] Skartveit-Olseth [16]	DISC-Hay DISC-Perez DISC-SO	Meteonorm [40]
BRL [13]	LiuJordan	BRL-LJ	Summa [41]

The goal of this study is to investigate 15 decomposition models partnered with transposition models which are integrated with feasibility software using a full year's worth of data, at φ = 51.1°. It analyses the errorbetween modelled and measured POA

irradiance. An overview of the methodology used to estimate POA is provided in this paper. The description of the different tilted components that make up the POA will be introduced, using GHI for the reflected component (R_T), DNI for the beam component (B_T), and DHI from the decomposition model. Afterward, the diffuse tilted component (D_T) is acquired by transposing them. To facilitate the review of the distinct optical model pairings, the sky clarity is divided into clear, intermediate, and overcast categories.

Firstly, the error in the 15 optical model pairs for a tracked and FT system concerning diverse sky conditions is analysed. This analysis can highlight discrepancies derived from overpredicting or underpredicting DHI, subsequently leading to a flawed representation of POA [21]. Furthermore, it is essential to quantify which factor has a more pronounced impact on the model performance: decomposition or transposition. After choosing the best-performing pair among the 15, which showed minimal error, this model is used to assess the performance of the optical model pair in a tracking system. The aim is to map horizontal irradiance minutely and convert these measurements to POA irradiance under varying weather conditions. The concluding assessment is to examine the impact of temporal resolution on the top-performing model pair. By comparing the error percentages between hourly and minute-by-minute data inputs, it can be determined whether high temporal resolution data yields consistent results

III. METHODOLOGY

A. Models

A total of 5 distinct decomposition models are in use (see Table 1) [9-13]. All of these models rely significantly on the sky clearness index (K_t) for assessing sky conditions, which is derived by taking the ratio of the GHI to the extraterrestrial horizontal irradiance, E_a, as depicted in equation 1.

$$K_t = \frac{GHI}{E_a} \tag{1}$$

$$GHI = DHI + DNI\cos(SZA) \tag{2}$$

The DIRINT and DISC models [46] utilize GHI and K_t, among other parameters (i.e., dew point temperature). Moreover, the BRL model incorporates the Zenith angle (SZA) and the apparent solar time. Both models yield DNI rather than DHI, but regardless, all decomposition models effectively generate estimates of both DHI and DNI for conversion using the closure equation in Equation 2.

POA irradiance is then estimated using D_T with B_T and R_T as per Equation 3, with B_T calculated using the angle of incidence (AOI) and DNI (Equation 4). The 7 transposition models listed calculate D_T [14-20]. These models vary in complexity, ranging from a basic isotropic representation of the sky (LJ [15]) to complex empirical correlations incorporating look-up table integrations, as in the Perez model.

$$POA = B_T + D_T + R_T \tag{3}$$

$$B_T = DNI\cos(AOI) \tag{4}$$

As for R_T, it operates under isotropic conditions, signifying that all rays maintain uniform intensity (see equation 5).

$$R_T = GHI \cdot \rho \cdot \left(\frac{1-\cos(\beta)}{2}\right) \tag{5}$$

The simplistic reflection of ground rays is processed as though from a Lambertian surface, where the quantity of ground re-emission depends on the albedo (ρ) [68]. For the purpose of this study, given the presence of grass on the site, ρ was set at 0.20. This value aligns with the default value for vegetated terrains in feasibility software [27]. Furthermore, the assumption here is that the foreground is infinitely extensive and unobstructed by shade. However, it should be noted that ρ varies based on numerous factors, such as the nature of the surface, i.e. whether it is a water-logged surface following rain, or simply an expanse of green grass. This variation could lead to compensatory or augmentative effects on error relative to other uncertainty
sources in the optical model pair. As a result, the reliance on reflected irradiance remains unchanged and is set as the default in feasibility software.

B. System Configuration

Table 2: Specifications of the actuator-based tracker and the FT system.

System	Type	Experimental Duration	ψ_{system} (°)	β (°)
1	Tracker	Apr 14 2023 – Apr 13 2024	126 -247	33 - 68
2	FT		180	55

The tracker in this study uses an actuator control system to adjust the solar panel array's tilt angle along the East-West axis. It aligns the panels based on the sun's altitude and azimuth within a two-dimensional coordinate system. Due to limitations in actuator

lengths, the system consistently aims the panels at the sun within predefined boundaries during its tracking cycle, as detailed in Table 2.

The study utilized Spectrally Flat Class A pyranometers (CMP10) to measure POA and GHI, in accordance with the International Electrotechnical Commission (IEC) 61724 standards [26]. These standards encompass everything from calibration to sensor placement, ensuring consistent and accurate data collection. Further, the examination of the optical model pairs is also performed at one-minute intervals, an approach designed to seize the variety inherent in the tracking combinations (i.e., $\beta - \psi_{system}$) that an hourly computation would not facilitate [47].

C. Sky Categorisation

Table 3: Sky conditions and corresponding sky clarity ranges.

Sky Condition	Range
Overcast	$K_t < 0.30$
Intermediate	$0.30 \leq K_t \leq 0.68$
Clear	$K_t > 0.68$

The classification of sky conditions into clear and overcast conditions is achieved via Equation 1, utilizing NREL's Solar Positon Algorithm (SPA) [30] to ascertain the solar position. Page et al. noted the typical decrease in K_t values at higher φ, and provided ranges for sky classification in the context of the UK climate, as illustrated in Table 3 [31]. The computations were based using equation 1 corresponding to the φ under investigation. SZA was kept under the limit of 75°, and a daily K_t average was obtained to minimize errors attributable to the uncertainty threshold of the pyranometers.

Employing the average K_t permits each day to be classified under a specific condition. At φ = 51.1°, where the prevailing K_t was found to be 0.48, clear conditions were observed on 31 of the 364 days, with an average K_t of 0.70, while overcast conditions (average K_t = 0.19) were reported on 101 days.

D. Employing the Error Threshold

The uncertainty in the energy output over time, as well as the error in determining the best design parameters of PV systems, heavily depends on the accuracy of the incident irradiance measurements or models. Therefore, the purpose is to assess the performance of various optical model pairs in estimating the POA irradiance. Therefore, a benchmark was set for the Mean Absolute Error (MAE) of <5%. MAE is depicted in Equation 6. Here, POA_M refers to the measured POA irradiance from the pyranometer, whereas POA_S pertains to the modelled POA irradiance calculated using the decomposition-transposition model pair for the *i*-th data point. The number of data points is depicted as *n*.

$$Mean\ Absolute\ Error\ (\%) = \frac{1}{n}\sum_{i=1}^{n}\left|\frac{POA_M - POA_S}{POA_M}\right| \times 100 \qquad (6)$$

E. Limitations of the Presented Study

The pyranometers (having an uncertainty of ±1.44%) used are calibrated under specific conditions (i.e., SZA ≈45°) leading to increased measurement uncertainty during periods of low irradiance, such as overcast conditions. This may affect the accuracy of the data gathered, especially when solar irradiance is diminished. Additionally, this study did not incorporate ρ measurements but instead specified a constant ρ = 0.20 for grassy surfaces within the feasibility software. This could influence the comparative performance of the model pairs, particularly the FT system which is affected by its steep AOI. Unfortunately, this limitation is dictated by the constraints of the feasibility software, hence its adoption in our methodology. Moreover, the results presented here are based on standalone data from a single location. Another drawback is that the measurements focus solely on global in-plane POA, excluding diffuse and/or direct. This exclusion makes it challenging to determine the extent to which DHI or DNI contribute to errors in the analysis of in-plane POA.

Aligning pyranometers with the POA is challenging, often resulting in alignment errors of several degrees. These errors increase as the AOI to the POA widens. Consequently, systems with a lower AOI, such as the tracker system, tend to exhibit fewer errors percentage from POA and pyranometer misalignment compared to FT system. However, it's important to acknowledge the impact of different elevation heights and the inherent nature of movement in tracking systems contributing to unavoidable errors in systems with varying AOI.

IV. Results And Discussion

A. Examining Pairs in Clear Conditions

The percentage errors for the 15 model pairs, across the three conditions for both the tracked and FT systems, are presented in Table 4. The performance seems to hinge on the fundamental aspects of either the initiation of the decomposition segment or the implementation of the transposition component within the optical model combination. A total of 4 models conform to MAE < 5% for the FT setup, with MAE fluctuating between 3.21% and 25.45%.

Both Erbs and Reindl employ similar equations, exhibiting a negative linear gradient for the latter and a negative exponential-like shape for the former in clear instances. Comparing Erbs-Perez and Reindl-Perez, it is evident that their errors to measurement are closely aligned at 5.11% and 3.21%, respectively. The same can be observed with Skartviet Olseth (referred to as SO), where the Erbs model results in MAE of 17.25% and the Reindl model yields 14.88%.

Table 4: The performance of 15 different decomposition-transposition model pairs is evaluated across clear, intermediate, and overcast conditions. Green highlights signify the pair meets the specified threshold MAE < 5%.

POA Error (%)						
Combination	Clear		Intermeidate		Overcast	
	Tracker	FT	Tracker	FT	Tracker	FT
BRL-LJ	3.70	7.44	7.20	10.81	4.81	7.42
DIRINT-Perez	2.82	4.96	3.28	5.53	45.22	31.73
DISC-Hay	3.94	6.80	6.18	5.89	5.72	7.28
DISC-Perez	2.78	3.73	3.31	4.99	44.56	30.23
DISC-SO	3.31	3.22	3.12	2.87	3.23	2.67
Erbs-Bugler	8.08	15.27	6.24	10.39	10.69	10.82
Erbs-Hay	4.17	10.60	6.93	6.10	7.08	8.86
Erbs-LJ	3.42	11.03	5.62	9.23	5.05	7.02
Erbs-Perez	4.97	5.11	4.37	8.91	38.81	26.79
Erbs-SO	6.00	17.25	5.73	10.93	8.90	10.93
Erbs-TC	8.36	16.44	12.95	19.35	51.07	40.47
Erbs-Willmot	13.92	25.45	7.14	17.31	37.66	8.73
Reindl-Hay	4.79	15.01	5.20	11.01	13.01	12.25
Reindl-Perez	4.41	3.21	3.33	9.09	35.95	25.76
Reindl-SO	7.70	14.88	6.44	9.72	9.30	6.72

Examining the empirical origins of transposition models reveals insights into their performance. For example, the Bugler model defines sky clarity using DHI, making DHI computation integral to transposition. This accounts for the error of 15.27% in the FT system, due to the lower number of cos(AOI). At higher values of cos(AOI), like that of the tracker, the percentage error is lower by nearly half, at 8.08%. Similarly, the Temp-Coulson (TC) model also includes the cos(AOI) but raises it to a power of two and a cubic function of sin(SZA). This explains the better performance of that model for the tracker (8.36%) compared with the FT system 16.44%). The Willmot model employs an empirical quadratic equation as a function of β. Thus, a FT outside of its empirical range (i.e., $\beta = 55°$) results in a high percentage error from measurement (25.45%). On a tracker, though still large, the error for Erbs-Willmot is reduced to 13.92%.

For the tracker, 10 of the 15 models conform to the figure of merit. Using a simple isotropic transposition model (in this case, Liu-Jordan or LJ) offers a more accurate portrayal of POA; mainly due to DHI being minimal, resulting in a low error from the measurement. Still, all models using Perez as the transposition part, adhere to the threshold, albeit producing overestimations rather than underestimations possibly due to the mathematical contributions of the model coefficients of the sky clearness bins found within the lookup table of the Perez model.

B. Examining Pairs in Overcast Conditions

Overcast conditions, by their nature, imply that a considerable segment of total irradiance will originate from DHI. Hence, the role of decomposition models becomes similar to their function in clear conditions but reversed - now focusing on D_T. According to Table 4, all combinations for the FT system except for the DISC-SO pair have MAE >5%. Moreover, the range of percentage errors for the tracked system extends from 3.23% to 51.07%, while for FT, it spans 2.67% to 40.47%. For the tracked system, the number of models meeting the error threshold in overcast conditions decreased from 10 to 2. This reduction is primarily because the function of cos(AOI) nears one in clear conditions, where B_T dominates. Notably, employing LJ in the transposition role performs similarly in overcast conditions. Comparing BRL-LJ and Erbs-LJ, both assume D_T computation is uniformly distributed over the sky and their percentage errors to the measurement for the tracked system are quite similar, with a difference of only 0.24%. This further validates the use of isotropic models under overcast conditions, where diffuse irradiance scatters homogeneously.

The only model pair within the established threshold in both systems is the DISC-SO combination. However, it is important to note that the optimal estimation of DHI does not necessarily come from the DISC among the 5 decomposition models, as other transposition models using DISC still display substantial errors from the measured POA. In addition, regardless of the decomposition model used or the system type examined, combinations incorporating Perez consistently perform poorly. Extreme

MAE ranges from 25.76% to 45.22%, possibly due to unsuitable constants defined in the lookup function for low sky brightness coefficients, suggesting a calibration necessity. The TC transposition model also presents the most significant POA percentage errors in both systems, with 51.07% for the tracker and 40.47% for the FT setup, respectively. The cause of this low performance is not attributed to the Erbs component, but primarily to the transposition aspect. The methodology is simplified, which can lead to inadequate results when horizons are darker during overcast conditions. The TC model results from an integrated segment of the sky, exposed to these specified $\beta - \psi_{system}$ combinations. However, only a limited set of measurements from the 49 combinations in clear skies were taken, specifically from late January to early April at a $\varphi < 50°$.

C. Examining Pairs in Intermediate Conditions

Similar to the conditions of both clear and overcast conditions, the number of model pairs meeting the threshold is higher in the tracked system compared to the FT setup. The tracked system features 5 model pairs with MAE within 5%, while the FT system includes only 2. For the FT system, these are DISC-Perez, which falls just 0.01% within the threshold, and DISC-SO with MAE of 2.87%. Meanwhile, the tracked system also includes these two pairs, in addition to DIRINT, DISC, and Reindl paired with Perez.

The Erbs-Willmot and Erbs-TC model combinations had the most significant percentage errors relative to the measured POA. The former had 7.14% and 17.31% for the tracker and FT system, respectively, while the latter combination showcased a percentage variance of 12.95% and 19.35%. The TC model employs trigonometric principles to track D_T variability rooted in solar position, while the Willmot model showcases a modification of the Hay model, incorporating its unique sky clarity definition and a second-order polynomial as a function of β. The conception of both the Willmot and TC models accepts that enhancements can better the approximations for dispersed clouds, as brightening on the horizon in these circumstances stem from a seemingly larger sky coverage due to clouds overlapping near the horizon. Naturally, the error percentage of Willmot and TC is reduced in a tracked system because the $\beta - \psi_{system}$ leads to angles upon which they have been validated. A certain consistency is noticeable when the Perez transposition model is applied. In the tracked system, the discrepancy between models employing Perez is marginal, with only a difference of 1.09% between the highest and lowest MAE (i.e., all fall within the 3.38% to 4.37% margin). However, the FT system does not exhibit a similar pattern, having a more significant percentage difference; i.e., 4.10% between 4.99% and 9.09%. This may suggest that the Perez model functions well under intermediate conditions and that with accurate DHI estimation, it may yield smaller percentage differences. Its coefficients seem better suited due to two primary factors: the selected coefficients align better with the average intermediate sky, and the SZA parameter may inadvertently contribute to intermediate conditions being aligned with brightness coefficients.

Moreover, during intermediate conditions, which account for the majority of the experiment's duration with an average K_t of 0.48, the roles of the decomposition and transposition models become equivalent as both B_T and D_T contribute similarly to the POA. For the tracked system, employing an isotropic transposition model (LJ) leads to an overestimation of 7.20% if BRL is the

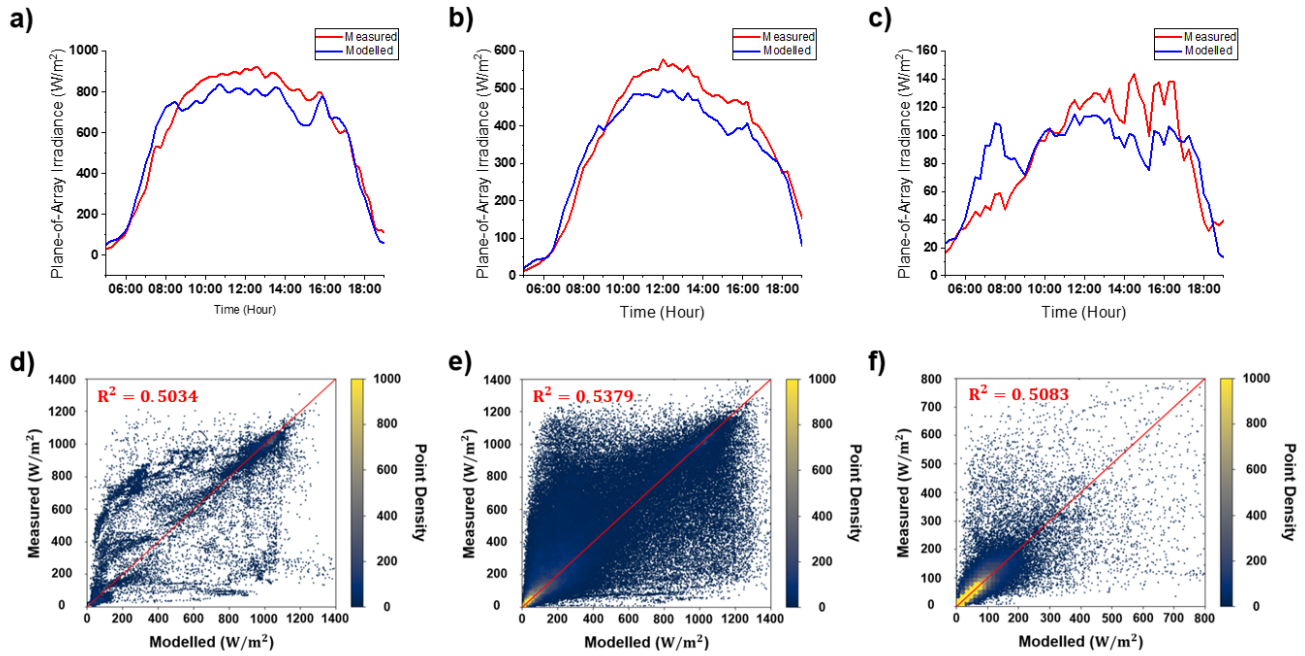

Figure 1: The given illustration shows a side-by-side comparison of POA irradiance recorded every minute but displayed in 15-minute slots against the time of day. This includes both measured and the DISC-SO model for the tracked system under clear **(a)**, intermediate **(b)**, and overcast **(c)** conditions. Additionally, a scatter plot provides a comparison of per-minute irradiance over the selected period between the measured and modelled POA for clear **(d)**, intermediate **(e)**, and overcast **(f)** conditions. The R^2 values show the coefficient of determination.

decomposition basis or 5.62% if Erbs is chosen. By assuming an isotropic sky, models can effectively capture scattering. However, FT showcases a two-fold increase in MAE from measurement with BRL-LJ and Erbs-LJ compared to its tracking counterpart as the tracker observes sky variations under different cloud accumulations owing to its $\beta - \psi_{system}$ combinations. The decomposition models used for LJ (i.e., Erbs and BRL) may require adjustments in intermediate conditions due to their inverse sigmoid function, elucidating the estimation sign change when transitioning to a tracking system. The DISC-SO pair indicates the most suitable performance across both systems.

D. An Analysis of Decomposition Against Transposition

Identifying appropriate irradiance models is critical, whether for transposition or decomposition purposes. It is particularly important to validate these models from various angles (i.e., through the use of a tracker). In terms of decomposition, when comparing measured DHI to modelled values, the Erbs and Reindl models displayed MAEs of 18.34% and 19.68%, respectively. The BRL model recorded an MAE of 9.02%, while the DISC and DIRINT models demonstrated lower MAEs of 6.89% and 6.56% respectively, attributed to their similar mathematical formulations and conceptual similarities.

Table 5: Across the 15 different optical models, the overall percentage error due to the effects of decomposition and transposition is presented. The percentage MAE for the fixed-tilt system is indicated in brackets, while the error for the tracked system is shown without brackets.

		Transposition						
		LJ	**Perez**	**Hay**	**SO**	**Bugler**	**TC**	**Willmot**
Decomposition	**BRL**	6.24 (9.58)	-	-	-	-	-	-
	Erbs	5.28 (8.77)	13.95 (13.54)	6.74 (7.25)	6.63 (11.47)	7.63 (10.92)	23.11 (24.95)	16.14 (15.63)
	DIRINT	-	14.85 (12.73)	-	-	-	-	-
	DISC	-	14.68 (11.37)	5.86 (6.35)	3.17 (2.84)	-	-	-
	Reindl	-	12.25 (13.20)	7.33 (11.69)	7.34 (9.33)	-	-	-

Transitioning to transposition evaluations, where models are compared against measured DAT POA data throughout the year, both the TC and Willmot models showed relatively high MAEs, with Willmot at 13.93% and TC at 13.10%. Employing a simplistic isotropic sky approximation (e.g., LJ model) resulted in an MAE of 6.75%, which does not effectively represent intermediate sky conditions as mirrored in Table 4. Moreover, the Bugler model showed an MAE of 3.59%. In contrast, the Perez model achieved a lower MAE of 2.51%, suggesting that it performs well overall in temperate climates due to its empirical coefficients. However, it may require additional validation and fine-tuning for overcast conditions. The Hay model had an MAE of 1.47%, and the SO model achieved the lowest MAE of 0.22%, indicating that Hay's adjustments to align with SO's empirical adjustment, suitable for temperate, high φ environments, are effective.

Several feasibility software programs integrate diverse methods that incorporate decomposition models to forecast DHI and then DNI (or the other way around), followed by transposing them. The examination underway investigates which factor plays a stronger role in percentage discrepancies: the decomposition or the transposition model. Table 5 presents the overall percentage error of the 15 model pairs on both systems. Notably, the variations display distinct percentage discrepancies. The decomposition model employed will contribute to this difference, but the transposition model implementation after the prediction of DHI (and DNI) proves to be crucial.

A closer analysis of various combinations indicates that the main variation stems from the choice of the transposition model, irrespective of the foundation of the decomposition model. For example, considering the Erbs, DISC, and Reindl models and pairing them with Perez, Hay, or SO reveals more apparent differences in the choice of transposition model than in the choice of decomposition model. Taking Erbs-Perez as a reference point: altering the decomposition model leads to a maximum variation of 2.43% for the tracked system and 2.17% for the FT system among the previously mentioned models. To further corroborate this, analyzing the DISC decomposition model combined with Hay, Perez, or SO shows a variation of 6.29% for the FT system and 7.32% for the tracker system across these three configurations. Moreover, using Hay for transposition while varying the decomposition models (such as DISC, Erbs, and Reindl) results in a 5.34% variation for the FT system and 1.47% for the tracker system yet again changing the transposition yields to a maximum difference of 11.51% for the tracker system and 8.53% for the FT system. In essence, while there is a discernible difference in selecting the decomposition model, it is not as pronounced as when choosing the transposition model. This can be attributed to the varied mathematical approaches used by the transposition model to estimate the diffuse component based on DHI data.

E. Assessing the efficacy of the optimal optical model

An important aspect of this section is to examine how well an optimal model combination performs. As noted in prior literature, it is imperative to examine the scalability of model pairs at different β - ψ_{system} combinations, thus this section's focus will be solely on the actuator-based tracker. Table 4 provides a comprehensive analysis, showing that the pairing of the DISC decomposition model with the SO transposition model results in the smallest percentage errors. The DISC model incorporates SZA, and the SO model, devised empirically at φ =60°, includes SZA in its equation in conjunction with the AOI. Figure 1 illustrates the comparison between measured and modelled data (DISC-SO), for varying sky conditions.

Figures 1a and 1b demonstrate a close alignment between the modelled and measured POA irradiance, mirroring similar fluctuations. This alignment suggests that while the model generally captures the irradiance profile, it occasionally diverges by overestimating or underestimating the POA. The coefficients of determination (R^2), 0.5034 for clear conditions and 0.5379 for intermediate suggest a scatter in the data points due to the high temporal resolution of the input data and hourly basis of the SO model's creation, particularly evident in Figure 1e, which shows dense clustering of data points from 0 to 200 W/m². In overcast conditions, as depicted in Figure 1f, there is an initial strong alignment in low irradiance readings, but less so at higher levels, explaining the low R^2 and variability.

F. Temporal Resolution Efffect

Solar radiation data is often required at intervals shorter than the typical hourly break. This demand becomes even more pressing in light of the volatile weather typical of temperate regions. Accurate irradiance estimation is crucial, especially in areas with significant variations in SZA. Using an hourly timeframe can compromise the reliability of these estimates. However, most decomposition and transposition models have been empirically developed using hourly data inputs. Hence, this study investigates the effectiveness of the DISC-SO when utilizing both hourly and minute-by-minute input data.

Figure 2: The Mean Absolute Error of the DISC-SO model pair for the tracked system, using solar irradiance inputs in both hourly and minute intervals, across different sky conditions.

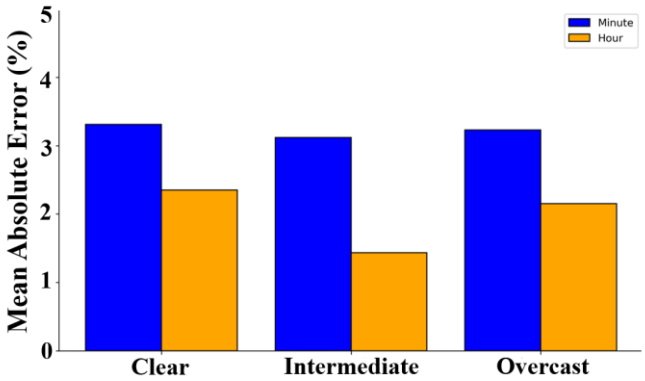

Across all the sky conditions, as evident in Figure 2, feeding hourly data into the decomposition and transposition contexts results in a lower MAE of the DISC-SO compared to the measured POA. The most significant difference occurs during intermediate conditions, where switching from hourly to minute data shows a error of 1.68%. Additionally, in overcast and clear conditions, opposite trends are observed. Specifically, under clear conditions, hourly data exhibit MAE of 2.35%, while minute data show 3.31%. Conversely, during overcast conditions, minute data results in an MAE of 3.23%, whereas hourly data has an MAE of 2.15%. These variations may be due to the overprediction of DHI at the minute scale, leading to underestimations in POA when transposed, and the reverse occurring under clear conditions with minute data.

The search for reliable decomposition models suitable for a wide range of φ within temperate regions remains critical. However, an even greater emphasis is placed on identifying suitable, robust transposition models, with the aim of designing a framework that seamlessly integrates both mathematical models for more accurate POA estimations. To accurately assess direct and diffuse plane POA, specialized instruments are essential. This involves using a pyranometer equipped with a shading disc for precise measurement of diffuse POA, alongside a pyrheliometer specifically designed to record in-plane direct POA. However, it's important to consider that the pyrheliometer's narrow half-angle of 2.5 degrees may introduce sensitivity issues, potentially impacting the accuracy of data under specific environmental conditions.

V. CONCLUSION

In conclusion, the study involved analysing 15 different optical model combinations within feasibility software, comparing them against measured POA for both a tracking and a south-facing tilted system set at 55° in a sub-hourly context. The error of the

model-derived POA from that derived from measurement (i.e., the error of the model) ranged drastically, from 2.67% to 51.07%, influenced by factors such as K_t and the type of system used. Evaluating the precision of these models, particularly when the mean absolute error (MAE) exceeded 5%, revealed inconsistencies across different sky conditions. Specifically, the number of model pairs meeting the threshold decreased with diminishing sky clarity: 10 pairs in clear skies (ranging from 2.78% to 4.97%), five pairs in intermediate conditions (from 3.12% to 4.37%), and only two pairs under overcast conditions (4.81% and 3.23%) for the tracking system. For the fixed tilt system, the numbers were five in clear conditions (from 3.21% to 4.96%) and two in intermediate conditions, dropping to just one, DISC-SO, in overcast conditions with an MAE of 2.67%. Furthermore, the impact of decomposition versus transposition was examined. While changes in decomposition resulted in a maximum percentage discrepancy of 2.43% for tracking systems and 5.34% for fixed-tilt systems, altering the transposition model led to a percentage error of 11.51% for tracking systems and 8.53% for fixed-tilt systems. Additionally, the DISC-SO pair was analyzed to assess the effect of temporal resolution in input solar irradiance data. It was found that using hourly input data resulted in lower MAE, with values of 1.44% under intermediate conditions, 2.15% in overcast conditions, and 2.35% in clear conditions, performing better than minute data. This may be due to the empirical definition of the model combination, as the models were developed using hourly data rather than minute data. Yet, there is a pressing need for irradiance estimations in the sub-hourly context. Given the varied estimation errors, future work should establish a robust benchmarking framework for selecting suitable decomposition models, and then coupling them with appropriate transposition models.

ACKNOWLEDGMENT

Y. J. K. Musleh and W. Herring acknowledge the support of the Engineering and Physical Sciences Research Council (EPSRC) Doctoral Training Partnership (DTP) Funding. S. A. Boden acknowledges support from EPSRC grant EP/S000763/1. T. Rahman acknowledges support from EPSRC grant EP/X033333/1. The authors would like to acknowledge the use of data from the radiometers at Chilbolton Atmospheric Observatory, collected as part of long-term measurements funded by UKRI-NERC National Capability. For the purpose of open access, the author has applied a Creative Commons Attribution (CC BY) licence to any Author Accepted Manuscript version arising.

REFERENCES

[1]: United Nations / Framework Convention on Climate Change. (2015). Adoption of the Paris Agreement, 21st Conference of the Parties, Paris: United Nations.
[2]: IPCC. (2022). Climate Change 2022: Impacts, Adaptation and Vulnerability. Contribution of Working Group II to the Sixth Assessment Report of the Intergovernmental Panel on Climate Change [H.-O. Pörtner, D.C. Roberts, M. Tignor, E.S. Poloczanska, K. Mintenbeck, A. Alegría, M. Craig, S. Langsdorf, S. Löschke, V. Möller, A. Okem, B. Rama (eds.)]. Cambridge University Press. Cambridge University Press, Cambridge, UK and New York, NY, USA, 3056 pp., doi:10.1017/9781009325844.
[3]: COP26: Key outcomes and next steps for the UK. (2021).
[4]: International Roadmap for Photovoltaic (ITRPV). (2022). 13th edition
[5]: R. Kopecek and J. Libal, "Bifacial Photovoltaics 2021: Status, Opportunities and Challenges," Energies, vol. 14, no. 8. MDPI AG, p. 2076, Apr. 08, 2021. doi: 10.3390/en14082076.

[6]: C. D. Rodríguez-Gallegos et al., "Global Techno-Economic Performance of Bifacial and Tracking Photovoltaic Systems," Joule, vol. 4, no. 7. Elsevier BV, pp. 1514–1541, Jul. 2020. doi: 10.1016/j.joule.2020.05.005.
[7]: C. A. Gueymard and J. A. Ruiz-Arias, "Extensive worldwide validation and climate sensitivity analysis of direct irradiance predictions from 1-min global irradiance," Solar Energy, vol. 128. Elsevier BV, pp. 1–30, Apr. 2016. doi: 10.1016/j.solener.2015.10.010.
[8]: C. A. Gueymard, "A review of validation methodologies and statistical performance indicators for modeled solar radiation data: Towards a better bankability of solar projects," Renewable and Sustainable Energy Reviews, vol. 39. Elsevier BV, pp. 1024–1034, Nov. 2014. doi: 10.1016/j.rser.2014.07.117
[9]: D. G. Erbs, S. A. Klein, and J. A. Duffie, "Estimation of the diffuse radiation fraction for hourly, daily and monthly-average global radiation," Solar Energy, vol. 28, no. 4. Elsevier BV, pp. 293–302, 1982. doi: 10.1016/0038-092x(82)90302-4.
[10]: D. T. Reindl, W. A. Beckman, and J. A. Duffie, "Diffuse fraction correlations," Solar Energy, vol. 45, no. 1. Elsevier BV, pp. 1–7, 1990. doi: 10.1016/0038-092x(90)90060-p.
[11]: Maxwell, E. L., "A Quasi-Physical Model for Converting Hourly Global Horizontal to Direct Normal Insolation", Technical Report No. SERI/TR-215-3087, Golden, CO: Solar Energy Research Institute, 1987.
[12]: Perez, R., P. Ineichen, E. Maxwell, R. Seals and A. Zelenka, (1992). "Dynamic Global-to-Direct Irradiance Conversion Models". ASHRAE Transactions-Research Series, pp. 354-369
[13]: J. Boland, J. Huang, and B. Ridley, "Decomposing global solar radiation into its direct and diffuse components," Renewable and Sustainable Energy Reviews, vol. 28. Elsevier BV, pp. 749–756, Dec. 2013. doi: 10.1016/j.rser.2013.08.023.
[14]: R. Perez, P. Ineichen, R. Seals, J. Michalsky, and R. Stewart, "Modeling daylight availability and irradiance components from direct and global irradiance," Solar Energy, vol. 44, no. 5. Elsevier BV, pp. 271–289, 1990. doi: 10.1016/0038-092x(90)90055-h.
[15]: B. Y. H. Liu and R. C. Jordan, "The long-term average performance of flat-plate solar-energy collectors," Solar Energy, vol. 7, no. 2. Elsevier BV, pp. 53–74, Apr. 1963. doi: 10.1016/0038- 092x(63)90006-9.
[16]: A. Skartveit and J. Asle Olseth, "Modelling slope irradiance at high latitudes," Solar Energy, vol. 36, no. 4. Elsevier BV, pp. 333–344, 1986. doi: 10.1016/0038-092x(86)90151-9.
[17]: R. C. Temps and K. L. Coulson, "Solar radiation incident upon slopes of different orientations," Solar Energy, vol. 19, no. 2. Elsevier BV, pp. 179–184, 1977. doi: 10.1016/0038-092x(77)90056-1.
[18]: C. J. Willmott, "On the climatic optimization of the tilt and azimuth of flat-plate solar collectors," Solar Energy, vol. 28, no. 3. Elsevier BV, pp. 205–216, 1982. doi: 10.1016/0038-092x(82)90159-1.
[19]: J. W. Bugler, "The determination of hourly insolation on an inclined plane using a diffuse irradiance model based on hourly measured global horizontal insolation," Solar Energy, vol. 19, no. 5. Elsevier BV, pp. 477–491, 1977. doi: 10.1016/0038-092x(77)90103-7.
[20]: Hay, J. (1979). Study of Shortwave Radiation on Non-horizontal Surfaces. Canadian Climate Centre Report, Downs View.
[21]: R. Moretón, E. Lorenzo, A. Pinto, J. Muñoz, and L. Narvarte, "From broadband horizontal to effective in-plane irradiation: A review of modelling and derived uncertainty for PV yield prediction," Renewable and Sustainable Energy Reviews, vol. 78. Elsevier BV, pp. 886–903, Oct. 2017. doi:10.1016/j.rser.2017.05.020.
[22]: T. Mahachi and A. J. Rix, "Evaluation of irradiance decomposition and transposition models for a region in South Africa Investigating the sensitivity of various diffuse radiation models," IECON 2016 - 42nd Annual Conference of the IEEE Industrial Electronics Society, Florence, Italy, 2016, pp. 3064-3069, doi: 10.1109/IECON.2016.7793897.
[23]: M. Lave, W. Hayes, A. Pohl and C. W. Hansen, "Evaluation of Global Horizontal Irradiance to Plane-of-Array Irradiance Models at Locations Across the United States," in IEEE Journal of Photovoltaics, vol. 5, no. 2, pp. 597-606, March 2015, doi: 10.1109/JPHOTOV.2015.2392938.

[24]: X. Sun, M. R. Khan, C. Deline, and M. A. Alam, “Optimization and performance of bifacial solar modules: A global perspective,” Applied Energy, vol. 212. Elsevier BV, pp. 1601–1610, Feb. 2018. doi: 10.1016/j.apenergy.2017.12.041.
[25]: C. D. Rodríguez-Gallegos, M. Bieri, O. Gandhi, J. P. Singh, T. Reindl, and S. K. Panda, “Monofacial vs bifacial Si-based PV modules: Which one is more cost-effective?,” Solar Energy, vol. 176. Elsevier BV, pp. 412–438, Dec. 2018. doi: 10.1016/j.solener.2018.10.012
[26]: International Electrotechnical Commission. (2021). IEC 61724-1: Photovoltaic system
performance - Part 1: Monitoring.
[27]: J. C. Blakesley et al., “Effective Spectral Albedo from Satellite Data for Bifacial Gain Calculations of PV Systems,” 37th European Photovoltaic Solar Energy Conference and Exhibition; 1292-1297, 2020, doi: 10.4229/EUPVSEC20202020-5CO.9.3.
[28]: Kipp & Zonen. (2015). CMP10 Pyranometer [Datasheet]. Retrieved from https://www.kippzonen.com/Product/276/CMP10-Pyranometer#.ZFuD0XbMJjU
[29]: Campbell Scientific, Inc. (2021). CR1000X Measurement and Control Datalogger [Datasheet]. Retrieved from https://www.campbellsci.com/cr1000x
[30]: I. Reda and A. Andreas, “Solar position algorithm for solar radiation applications,” Solar Energy, vol. 76, no. 5. Elsevier BV, pp. 577–589, 2004. doi: 10.1016/j.solener.2003.12.003.
[31]: J. Page, "Chapter II-1-A - The Role of Solar-Radiation Climatology in the Design of Photovoltaic Systems," in S. A. Kalogirou (Ed.), McEvoy's Handbook of Photovoltaics (Third Edition), Academic Press, 2018, pp. 601-670, ISBN: 9780128099216, doi: 10.1016/B978-0-12-809921-6.00016-1.
[32]: K. J. A. Revfeim, “A Simple Procedure for Estimating Global Daily Radiation on Any Surface,” Journal of Applied Meteorology, vol. 17, no. 8. American Meteorological Society, pp. 1126–1131, Aug. 1978. doi: 10.1175/1520-0450(1978)017<1126:aspfeg>2.0.co;2.
[33]: Logiciel Photovoltaïque. (2013). Pvsyst. Retrieved from https://www.pvsyst.com/
[34]: Insel Group AG. Retrieved from https://insel.eu/en/home_en.html
[35]: Natural Resources Canada. RETScreen. Retrieved from https://naturalresources.canada.ca/maps-tools-and-publications/tools/modelling-tools/retscreen/7465
[36]: Ross, M. M. D., Turcotte, D., & Fry, M. A. (2005). PVToolbox Simulation Output Compared with Monitored Data from PV Hybrid Test Bench. Proceedings of the 30th Annual Conference of the Solar Energy Society of Canada.
[37]: TRNSYS. Retrieved from https://www.trnsys.com/
[38]: SolarAnywhere. Retrieved from https://www.solaranywhere.com/
[39]: Solargis. Retrieved from https://solargis.com/
[40]: Meteonorm. Retrieved from https://meteonorm.com/en/
[41]: S. Summa, G. Remia, A. Sebastianelli, G. Coccia, and C. Di Perna, “Impact on Thermal Energy Needs Caused by the Use of Different Solar Irradiance Decomposition and Transposition Models: Application of EN ISO 52016-1 and EN ISO 52010-1 Standards for Five European Cities,” Energies, vol. 15, no. 23. MDPI AG, p. 8904, Nov. 25, 2022. doi: 10.3390/en15238904.
[42]: PVSOL Software. Retrieved from https://pvsol.software/en/
[43]: PVPS Task 1. (2022). TRENDS IN PHOTOVOLTAIC APPLICATIONS 2022 Task 1 Strategic PV Analysis and Outreach PVPS. Retrieved from www.iea-pvps.org
[44]: Y. F. Nassar, S. Y. Alsadi, H. J. El-Khozondar and S. S. Refaat, "Determination of the Most Accurate Horizontal to Tilted Sky-Diffuse Solar Irradiation Transposition Model for the Capital Cities in MENA Region," 2022 3rd International Conference on Smart Grid and Renewable Energy (SGRE), Doha, Qatar, 2022, pp. 1-6, doi: 10.1109/SGRE53517.2022.9774146.
[45]: J. Freeman, J. Whitmore, N. Blair and A. P. Dobos, "Validation of multiple tools for flat plate photovoltaic modeling against measured data," 2014 IEEE 40th Photovoltaic Specialist Conference (PVSC), Denver, CO, USA, 2014, pp. 1932-1937, doi: 10.1109/PVSC.2014.6925304.
[46]: W. F. Holmgren, C. W. Hansen, and M. A. Mikofski, ‘pvlib python: a python package for modeling solar energy systems’, Journal of Open Source Software, vol. 3, no. 29. The Open Journal, p. 884, Sep. 07, 2018. doi: 10.21105/joss.00884.
[47]: M. A. Mikofski, W. F. Holmgren, J. Newmiller and R. Kharait, "Effects of Solar Resource Sampling Rate and Averaging Interval on Hourly Modeling Errors," in IEEE Journal of Photovoltaics, vol. 13, no. 2, pp. 202-207, March 2023, doi: 10.1109/JPHOTOV.2023.3238512.
[48]: Y. Fan et al., "Evaluation of 12 Transposition Models Using Observations of Solar Radiation and Power Generation," in IEEE Journal of Photovoltaics, vol. 12, no. 1, pp. 444-452, Jan. 2022, doi: 10.1109/JPHOTOV.2021.3129704.
[49]: B. G. Pierce, J. L. Braid, J. S. Stein, J. Augustyn and D. Riley, "Solar Transposition Modeling via Deep Neural Networks With Sky Images," in IEEE Journal of Photovoltaics, vol. 12, no. 1, pp. 145-151, Jan. 2022, doi: 10.1109/JPHOTOV.2021.3120508.
[50]: J. F. Orgill and K. G. T. Hollands, ‘Correlation equation for hourly diffuse radiation on a horizontal surface’, Solar Energy, vol. 19, no. 4. Elsevier BV, pp. 357–359, 1977. doi: 10.1016/0038-092x(77)90006-8.
[51]: C. A. Gueymard, “Direct and indirect uncertainties in the prediction of tilted irradiance for solar engineering applications,” Solar Energy, vol. 83, no. 3. Elsevier BV, pp. 432–444, Mar. 2009. doi: 10.1016/j.solener.2008.11.004.
[52]: D. Yang, Z. Dong, A. Nobre, Y. S. Khoo, P. Jirutitijaroen, and W. M. Walsh, “Evaluation of transposition and decomposition models for converting global solar irradiance from tilted surface to horizontal in tropical regions,” Solar Energy, vol. 97. Elsevier BV, pp. 369–387, Nov. 2013. doi: 10.1016/j.solener.2013.08.033.
[53]: M. Hofmann and G. Seckmeyer, “Influence of Various Irradiance Models and Their Combination on Simulation Results of Photovoltaic Systems,” Energies, vol. 10, no. 10. MDPI AG, p. 1495, Sep. 26, 2017. doi: 10.3390/en10101495.
[54]: Y. J. K. Musleh and T. Rahman, “Predictive models for photosynthetic active radiation irradiance in temperate climates,” Renewable and Sustainable Energy Reviews, vol. 200. Elsevier BV, p. 114599, Aug. 2024. doi: 10.1016/j.rser.2024.114599.
[55]: M. Manni, A. Nocente, M. Bellmann, and G. Lobaccaro, “Multi-Stage Validation of a Solar Irradiance Model Chain: An Application at High Latitudes,” Sustainability, vol. 15, no. 4. MDPI AG, p. 2938, Feb. 06, 2023. doi: 10.3390/su15042938.
[56]: J. J. Roberts, A. A. Mendiburu Zevallos, and A. M. Cassula, “Assessment of photovoltaic performance models for system simulation,” Renewable and Sustainable Energy Reviews, vol. 72. Elsevier BV, pp. 1104–1123, May 2017. doi: 10.1016/j.rser.2016.10.022.